HAL open science

# Regeneration of an aged hydrodesulfurization catalyst : Conventional thermal vs non-thermal plasma technology

Hawraa Srour, Elodie Devers, Adrien Mekki-Berrada, Joumana Toufaily, Tayssir Hamieh, Catherine Batiot-Dupeyrat, Ludovic Pinard

## To cite this version:

Hawraa Srour, Elodie Devers, Adrien Mekki-Berrada, Joumana Toufaily, Tayssir Hamieh, et al.. Regeneration of an aged hydrodesulfurization catalyst : Conventional thermal vs non-thermal plasma technology. Fuel, 2021, 306, pp.121674. 10.1016/j.fuel.2021.121674 . hal-03597653

**HAL Id: hal-03597653**

**https://ifp.hal.science/hal-03597653v1**

Submitted on 22 Aug 2023

**HAL** is a multi-disciplinary open access archive for the deposit and dissemination of scientific research documents, whether they are published or not. The documents may come from teaching and research institutions in France or abroad, or from public or private research centers.

L'archive ouverte pluridisciplinaire **HAL**, est destinée au dépôt et à la diffusion de documents scientifiques de niveau recherche, publiés ou non, émanant des établissements d'enseignement et de recherche français ou étrangers, des laboratoires publics ou privés.

Distributed under a Creative Commons Attribution - NonCommercial 4.0 International License

Version of Record: https://www.sciencedirect.com/science/article/pii/S0016236121015556
Manuscript_a536a30104036489e417f8dd76efeede

# Regeneration of an Aged Hydrodesulfurization Catalyst: Conventional Thermal vs Non-Thermal Plasma Technology

Hawraa Srour [1], Elodie Devers [2], Adrien Mekki-Berrada [2], Joumana Toufaily[3], Tayssir Hamieh[3], Catherine Batiot-Dupeyrat[1] and Ludovic Pinard [1,*]

[1] Institut de Chimie des Milieux et Matériaux de Poitiers (IC2MP), UMR 7285 CNRS, 4 rue Michel Brunet, Bâtiment B27, TSA 51106, 86073 Poitiers Cedex 9 – France.
[2] IFP Energies nouvelles, Rond-point de l'échangeur de Solaize, BP 3, 69360 Solaize, France
[3] Laboratoire des matériaux, catalyse, environnement et méthodes analytiques (MCEMA), Université Libanaise, Liban

* Corresponding authors: ludovic.pinard@univ-poitiers.fr
catherine.batiot.dupeyrat@univ-poitiers.fr

## Abstract

This study compares the regeneration efficiency of an aged industrial hydrodesulfurization catalyst ($CoMoP/Al_2O_3$) by conventional and alternative routes: thermal oxidation versus non-thermal plasma technology (NTP). Spent, partially, and fully regenerated catalysts have been characterized by XRD, XPS, and toluene hydrogenation to measure hydrogenating activity. Complete regeneration of the HDS catalyst via NTP requires the heating of the dielectric barrier discharge plasma reactor. Total removal of coke is obtained from 250 °C by applying only 8.6 $W/g_{catalyst}$, against 400 °C by conventional thermal treatment. The hydrogenation activity of the regenerated catalyst by NTP assisted by temperature is higher than that obtained by traditional thermal regeneration practiced industrially. Plasma treatment mitigates the oxide sintering but leads to the formation of cobalt oxide species preventing Co of fully playing its role as $MoS_2$ slabs promoter. HDS catalyst regeneration using non-thermal plasma assisted by low temperature appears as a promising alternative to thermal combustion.

Keywords: HDS catalyst, thermal regeneration, non-thermal plasma, coke



© 2021 published by Elsevier. This manuscript is made available under the CC BY NC user license
https://creativecommons.org/licenses/by-nc/4.0/

## 1. Introduction

It is well known that air pollution is a severe environmental problem. The combustion of organosulfur and organonitrogen compounds present in feedstocks are responsible for the generation of atmospheric air pollutants such as SOx, NOx, and particulate matter. Consequently, hydrotreatment processes are required to remove such compounds before conversion into gas oil in refinery units. The sulfur content must be less than 10 ppm in commercial on-road gas oils [1].

The hydrodesulfurization (HDS) process is used to remove sulfur-containing compounds from gasoline and diesel fuels. The most widely employed catalyst for the hydrodesulfurization process is cobalt-molybdenum supported on alumina [2]. The industrial catalysts are relatively robust; for example, typical commercial HDS catalysts have a lifetime of 2–4 years in industrial applications [3]. However, deactivation is still a problem of great concern. The three typical causes of deactivation of hydroprocessing catalysts are coke, sintering, and contamination.

Coke deposition is one of the main reasons for the deactivation. Koh [4] identified two types of carbonaceous species deposited on the $CoMo/Al_2O_3$ catalyst in the HDS of dibenzothiophene (DBT): the reactive and the refractory species. The authors indicated that the refractory deposit, or hard coke, was a significant contributor to the deactivation. The alumina support is assumed to be rapidly covered by coke, while the active sites remain protected by their high hydrogenation activity [5].

The coke can be eliminated by regeneration, the ex-situ method being the rule nowadays for better performance recovery. Regeneration consists of controlled oxidation, which removes coke and converts sulfides back to oxides. Traditionally, the most widely used method for catalyst activity recovery is oxidative regeneration using diluted-air. The experimental conditions used were optimized and particularly in terms of temperature, as it must not exceed 500 °C to limit the formation of crystallized species such as $CoMoO_4$ or $CoAl_2O_4$ [6]. However, the presence of these phases is frequently observed after the regeneration step, while they are known to be refractory to sulfidation, influencing the HDS activity negatively [7].

The more recent works on catalyst regeneration are dealing with rejuvenation, i.e. reactivation using organic additives after thermic regeneration [8-9]. Recent works

start to deal with global cycle life of catalyst which of course include regeneration [10-11]

Consequently, there are needs to propose new strategies to perform catalyst regeneration. Among alternative processes and as indicated in the paper: “The 2020 plasma catalysis roadmap” [12], non-thermal plasma treatment appears as an effective technique for removing coke from various spent catalysts [13].

Under plasma containing oxygen, active species are produced, such as $O_2^+$, $O^-$, $O_2^-$ and $O_3^-$ [14], able to oxidize heavy molecules (graphitic or polyaromatic coke molecules [15] at atmospheric pressure and room temperature. The use of a Dielectric Barrier Discharge (DBD) plasma eliminated solid carbon of a Pt-Sn/$Al_2O_3$ catalyst using a pin to plate DBD plasma geometry [16]. A similar system was successfully used for the complete regeneration of coked zeolite [17, 18] and an industrial aged hydrotreating catalyst [19]. A coaxial DBD reactor is more suitable for an application of industrial scale. This configuration was also employed to regenerate a coked HFAU zeolite, and a kinetic study was performed, exhibiting the formation of carboxylic compounds as intermediates to $CO_2$ [205].

The efficiency of this alternative regeneration process depends strongly on the nature of coke. Higher character polycyclic compounds of the coke, lower their reactivity relative to the short-lived oxygenated species [20].

In this study, the regeneration of an aged industrial hydrodesulfurization catalyst was investigated in a fixed bed DBD plasma reactor. The plasma treatment was performed in the temperature range 70 to 300 °C since it has been shown that plasma is able to regenerate catalysts at temperatures lower than those of typical thermal regeneration [13]. The efficiency of the conventional and plasma routes will be compared in terms of recovery of toluene hydrogenation activity.

## 2. Experimental

The catalyst studied is a used industrial phosphorus-doped CoMoP/$Al_2O_3$ hydrotreatment catalyst, with the following mass composition 20.5%, $MoO_3$, 4.0% CoO, 5.2% $P_2O_5$. The surface area determined by the BET method is 145 $m^2/g$.

. It was recovered from a hydrodesulfurization process after two years on stream. Before any treatment, the catalyst was washed with toluene in a Soxhlet type device to extract the coke portion soluble in toluene (soft coke). The spent catalyst is

refluxed at 250 °C for 7 hours. The catalyst is then placed in a primary vacuum oven (30 mbar) at 150 °C for 3 hours. Before regeneration, spent catalysts were crushed and sieved to obtain homogeneous particles (0.1-0.2 mm).

The regeneration reactor is a cylindrical dielectric barrier discharge plasma reactor (DBD reactor) located in a furnace (**Figure 1** The temperature of the oven was regulated with a thermocouple at the inner wall of the oven. The Non-Thermal Plasma (NTP) reactor is made of an alumina tube of 6 mm of outer diameter. Alumina ceramic reactors were already used in various plasma applications due to their well-known long life, chemical stability, high hardness, temperature resistance [21-23]. The outer electrode, a copper sheet, is attached to the reactor by a special conductive glue. The inner electrode, a stainless steel rod (1.16 mm), is centred inside the reactor by a Teflon circle piece. Quartz wool folded around the inner electrode just under the plasma zone level holds the catalyst. The inner diameter of the reactor is 4 mm this corresponds to a gap of 1.42 mm. The plasma discharge is maintained in the zone between the two electrodes along 20 mm in length. The electrodes were connected to a high voltage (HV) sinusoidal generator. A low-frequency generator (GBF) from TTi® model TG1010A was coupled to a signal amplifier from TREK® model 30 / 20A. The signal delivered by the GBF is sinusoidal. The amplifier increases the voltage supplied by the GBF (x 3000 peak to peak), allowing it to work at high voltages. Power is supplied by coupling the low frequency generator and the amplifier. The high voltage is transmitted to the central electrode, located in the reactor, through a long shielded cable. The deposited power was measured by Q-U Lissajous method [24].

Non-thermal plasma regeneration (**NTP-R**) was carried out with gas feed composed of 20 vol% $O_2$ in He. Helium promotes energy transfer through the Penning effect to increase the concentration of active oxygen species ($O_2^+$, $O^-$, $O_2^-$ and $O_3$) in the gas phase [17-20]. The GHSV through the plasma reactor, calculated at 20 °C and 1 atm, was fixed to 6 000 $h^{-1}$, and the catalyst mass used is 350 mg. **NTP-R** was carried out at an input temperature of 70, 150, 200, and 300 °C. The catalytic bed temperature was measured with optic fiber in contact catalyst (Figure 1), and it was observed that it reaches approximately 100 °C when 70°C was applied and was not significantly modified for 150 °C and higher input temperatures because to the regulation of oven which takes account additional heat from NTP

The gas flow composition after the reactor was determined by on-line gas chromatographic analysis (Micro GC Varian CP 4900) equipped with a TCD detector, using a "COx column." Only $CO_2$ and CO are measured, the organic molecules (VOC) and water are trapped upstream of the µGC in order to protect it.

Thermal regeneration was carried out in the DBD plasma reactor (**$TR_{DBD\ reactor}$**) through a fixed bed in the same operating conditions (20% vol $O_2$, GHSV= 6000 $h^{-1}$, $m_{catalyst}$ =350 mg) as these used for the plasma regeneration, except that the generator is turned off. The temperature of the oven is fixed at 320, 350, 380, and 450 °C.

Optimized thermal regeneration (**O-TR**) consists of controlled combustion by injecting oxygen through a solenoid valve. The spent catalyst is placed in a vertical furnace under nitrogen flow ($6L.h^{-1}.g^{-1}$). The heating ramp is set at 5°C/min until 250 °C ±10 °C is reached. The oxygen flow rate is then adjusted to inject 5% vol. of oxygen. If the exothermicity exceeds 2 °C, the solenoid valve closes automatically, and the catalyst is flushed with nitrogen only. The oxygen injection only resumes when the temperature has dropped to 250 °C under 5% vol., 10% vol. Oxygen is injected, and when there is no more exothermicity at 250 °C under this condition, the oxygen feed is stopped. The catalyst is heated under nitrogen to the next temperature (maximum 50 °C) at the desired temperature; the oxygen injections start again under the same conditions as before. The catalyst is regenerated at different temperatures between 300 and 450 °C.

The amount of carbon and sulfur of the spent, partially, and fully regenerated catalysts was measured using a C.E. Instruments NA2100 PROTEIN elementary analyser.

X-ray diffraction patterns of the fresh, spent, and partially regenerated catalysts were recorded using a Malvern Panlytical ®, Empyrean model diffractometer operating with Cu K$\alpha$1 (radiation (l=0.15406 nm ) in the range of 10° <2$\theta$ < 80° with a step of 0.04° using a zero background holder with a 32 mm diameter.

XPS characterizations were made on the catalysts after the toluene hydrogenation catalytic test (see more below). The XPS sampling of the

catalysts was performed in a glove box under an argon atmosphere to prevent the partial reoxidation of $MoS_2$ nanocrystallites. The samples were crushed and pressed onto an indium foil on the sample holder and moved to the introduction chamber of the XPS spectrometer. The XPS spectra were recorded on a Kratos Axis Supra instrument assembled with an aluminum monochromator source (1486.6 eV) and a hemispherical analyzer functioning at fixed pass energy of 20 eV. The measurements were made at 20 °C in steps of 0.1 eV for cobalt, 0.1 eV for sulfur, and 0.1 eV for molybdenum, and at a pressure lower than 10-12 bar in the sample analysis chamber. C 1s peak at 284.6 eV was used as an internal standard for binding energy calibration. The curves were integrated by applying a Shirley type baseline. The collected spectra were analyzed by using Plug Im! software. The decomposition of the S 2p, Mo 3d and Co 2p signals was performed using the appropriate oxide and sulfided references as supported monometallic catalysts and according to the methods already described, and particularly to quantify the promoted CoMoS phase [25-26]. The Mo 3d spectra of sulfided catalysts were first decomposed (**Figure 2a**). Three different oxidation degrees of molybdenum were found: $Mo^{+VI}$ (232.2 eV), $Mo^{+V}$ ($MoS_xO_y$, 229.8 eV), and $Mo^{+IV}$ ($MoS_2$, 228.7 eV). They were, respectively, attributed to the oxide, oxysulfide, and sulfide phases. We then fixed a gap of 549.95 eV between $MoS_2$ and CoMoS and 0.49 eV between CoMoS and $Co_9S_8$, the third contribution being the cobalt oxide, which has to be integrated to correctly fit the spectrum (+/0.5 eV). (**Figure 2b**)

Similarly, the decomposition of the S 2p reveals three components, corresponding to three local environments: $S_{Sulf}$ (fully sulfided), $SO_x$ (oxysulfide species), and $S_{Sulfates}$ (fully oxidized) ). The fully oxidized form of S detected here is due to the partial exposure of the sample to air while transferring it to the XPS sampling chamber

The XPS decomposition led to the quantification of the relative amount of each species as follows:

$$[j] = \frac{A_j/S_J}{\sum_{i=1}^{i=n} A_i/S_i} \times 100 \qquad \text{(Eq.1)}$$

where $A_i$ is the measured area of each species, $S_i$ is the sensitivity factor for the atom related to the species i. [j] is the relative amounts of the various species.

The molybdenum sulfidation rate (SR) is calculated by assuming that all Mo is transformed into $MoS_2$. Mo SR is defined as

$$MoSR = \frac{[MoS_2]}{[Mo]} \times 100 \qquad \text{(Eq.2)}$$

The ratio of Co/Mo in the sheets $(Co/Mo)_{sheet}$ is calculated as:

$$\left(\frac{Co}{Mo}\right)_{sheet} = \frac{[CoMoS]}{[MoS_2]} \qquad \text{(Eq.3)}$$

The impact of regeneration on catalytic performances was evaluated in toluene hydrogenation reaction using a fixed bed unit reactor Flowrence rom Avantium. This reaction is considered as a model reaction for HDS catalyst since the most refractory species such as 4,6DMDBT react according to two main paths, the direct desulfurization (DDS) and the hydrogen path (HYD). This last one need the hydrogenation of aromatic rings before the rupture of the C-S bond and is the main path as described in Pérot, G. et al. [27]. As a consequence, using Toluene hydrogenation in presence of DMDS is a suitable model reaction. The main products are Methylcyclohexane, Ethylcyclopentane and Dimethylcyclopentane.

The reactor was filled with 450 µL of the catalyst diluted in Zirblast®. The feed was composed of dimethyldisulfide (DMDS, 5.8 wt%) and toluene (20 wt%) in cyclohexane (74.2 wt%). The hydrogen to feed ratio ($H_2$/HC) was kept at 450 $NL.L^{-1}$ during the test and the in-situ presulfidation step, which was performed at a liquid hourly space velocity (LHSV) of 4 $h^{-1}$ with a total pressure of 60 bar for 2 h. The temperature was increased from room temperature to 350 °C with a ramp of 2°C $min^{-1}$. After this presulfidation step, LHSV was turned down to 2 $h^{-1}$. The liquid products of the reaction at different temperatures were analyzed by gas chromatography using a DB1 column. The first-order rate constant (k, $h^{-1}$) was calculated by the following expression:

$$k'_{regenerated\ catalyst} = LHSV * \ln\left(\frac{1}{1-x}\right), LHSV = \frac{flow\ rate\ of\ the\ liquid\ feed}{volume\ of\ the\ catalyst} \qquad \text{(Eq. 4)}$$

x is the percentage conversion of toluene (HYD) in the feed. LHSV is the liquid hourly space velocity ($h^{-1}$). All the catalytic results will then be expressed as the Relative Volumic Activity $RVA(HYD)$, the industrial regenerated catalyst activity being the reference, according to the following equation :

$$RVA(HYD) = \frac{k'_{regenerated\ catalyst}}{k'indus\ rege\ catalyst\ (internal\ reference)} \qquad \text{(Eq. 5)}$$

## 3. Results and discussion

### 3.1. Conventional regeneration method ($TR_{DBD\ reactor}$)

The carbon and sulfur contents on the spent catalyst, determined by elementary analysis, are 13.0 and 8.8 wt. %, respectively. Sulfur derives largely from the remaining sulfur phase , i.e., CoMoS, $MoS_2$, $Co_9S_8$ [28].

The thermal regeneration of the spent catalyst was carried out under 100 $mL.min^{-1}$ airflow at a range of temperature 320-450 °C. **Figure 3** shows the cumulative yields of $CO_2$ and CO as a function of the treatment time at different temperatures and the relative C and S removals measured by elemental analysis after 1 hour. Regardless of the protocols used for thermal regeneration: fixed bed (**$TR_{DBD\ reactor}$**) reactor, with (**O-TR**) or without isothermal conditions, coke and sulfur removal rates are similar.

Cumulated yields into $CO_2$ measured for **$TR_{DBD\ reactor}$** exhibit a rapid and high increase as soon as the fixed temperature is reached (corresponding to point 0), exhibiting a plateau after 20 minutes of thermal treatment at 380 and 450 °C while the yield into $CO_x$ still increases until 60 minutes at the lowest temperature, 320 and 350 °C. (**Figure 3a**). It is probably due to the reaction's exothermicity, which significantly increases the temperature into the catalytic bed. Comparing the yield into $CO_x$ with C removal determined after regeneration (**Figure 3b**), it can be observed that the carbon balance is incomplete, whatever the temperature. The amount of C removed as $CO_x$ reaches 85 % at 450 °C, proving that heavy coke molecules are not selective into $CO_x$. This partial selectivity means that one part of the coke molecules is oxidized into desorbed products that are not detected, assumed as intermediate products [18-20].

It is confirmed that it is easier to remove sulfur than carbon under thermal treatments [5]. Probably, the location of a large portion of sulfur on the metallic phase as $MoS_2$ slabs facilitates its oxidation. A significant quantity (75 %) of sulfur was eliminated at the lower temperature, 320 °C.

**Figure 4** shows XRD patterns of the spent catalyst and the thermally treated samples at different temperatures. For the spent catalyst, $Al_2O_3$ Bragg peaks are recognized

at 2Θ= 33.4°, 37°, 39.5°, 46.1°, 66.7° and $MoS_2$ at 59°. The TEM Micrograph of the spent catalyst before treatment (**Figure 5**) displays black thread-like fringes, which corresponds to the structure of molybdenum disulfide $MoS_2$ slabs [5]. The $MoS_2$ slabs are randomly oriented and homogeneous distributed on the alumina support. Regardless of the thermal treatment, $Al_2O_3$ Bragg peaks are always detected. However, the patterns exhibit high noise leading to undefined signals. Starting from 300 °C, the Bragg peaks assigned to $MoS_2$ disappeared, in coherence with S removal. At high temperature, 500 °C, a new range of peaks appeared between 2θ = 26.5° and 39.5°, assigned to $CoMoO_4$; which are species refractory to sulfidation [29]. This is paired with the sintering effect and could be attributed to the aggregates (Al, O, P, Co, Mo) observed by TEM at 500 °C **Figure 5**).

### 3.2. Regeneration by non-thermal plasma (NTP-R)

The coked catalyst was treated by plasma in the temperature range: 70-300 °C. Experiments were performed to keep the frequency at 2 kHz, while the applied voltage varied from 7 to 12kV. As expected, the deposited power increases with the applied voltage regardless of the temperature (**Figure 6a**). With the increase in temperature, a shift in the breakdown voltage to lower values is observed. At 70 °C, the plasma appears from 9 kV, while only 6.5 kV is enough at 300 °C. Otherwise, to obtain an applied power of 5 W, an input voltage of 11.6 kV is needed at 70 °C, while 7.2 kV at 300 °C. The power depends on both the input voltage and the temperature (see Lissajous Figures in SI). Higher the temperature, lower the gas density, and higher the power [30].

As a corresponding sum up of these operational results, **Figure 6b** allows selecting the suitable operating conditions (U, T, P) to progress the study of iso-power plots, making it possible to know the value of input voltage needed to deposit an applied power ($P_A$) at a specific temperature. Therefore in this article, the results will be measured using a chosen $P_A$.

**Figure 7** shows the light-off curves of C and S removals, the yield into COx, and carbon balance as a function of the temperature under plasma-assisted by temperature (**NTP-R**) at different applied power ($P_A$). This data is compared with the

relative thermal treatment evolutions. With **NTP-R**, up to 150 °C, there is no significant modification of the C removal by temperature (**Figure 7a**) with C removal depending only on the amount of active species generated ($P_A$). From 200 °C, there is a rapid increase in C removal, which becomes total at 300 °C, regardless of the $P_A$ (**Figure 7a**). By opposition, S removal (**Figure 7b**) appears more sensitive to temperature, with a constant increase starting from low temperatures. These results show that the regeneration of HDS catalysts via NTP need to be temperature assisted. At a fixed temperature, both C and S removals are proportional to the $P_A$ (**Figures 8a and 8b**). In opposition to thermal treatment plasma promotes easier C removal than S removal at a lower temperature (**Figures 7 and 8**). Indeed, the most significant benefit of **NTP-R** is the lower temperature needed to reach total C and S removals. A gap of ΔT=100 °C at a range of $P_A$ of 2W-6W, and ΔT= 200 °C at a $P_A$ of 7W were observed (**Figures. 7a and 7b**).

Regardless of temperature and $P_A$, the yield of $CO_x$ is always lower than C removal (**Figures 7c and 8c**).This difference indicates that C balance (**Figure 6d**) for **NTP-R** is incomplete as observed with thermal treatment. It was observed that C balance depends mainly on the applied temperature (**Figure 7d**), the higher the temperature, the higher the carbon balance. Unfortunately , XRD evidences traces of $CoMoO_4$ formation even at 200°C under plasma discharge (**Figure 4**).

From the collected data, it is possible to calculate apparent activation energy ($E_a$) using Arrhenius law (**Figures 9a and 9b)**. The -Ln(C removal) and -ln(S removal) plots exhibit straight lines with a proportional linear increase as a function of 1/T at the different $P_A$. The equivalent slopes, which are equal to ($-E_a/R$), increase with the decrease in the $P_A$ in **NTP-R** treatments, with a higher slope in the case of thermal treatment. **Figure 10** reports the $E_a$ of C and S removals as a function of the $P_A$ for **NTP-R** compared to the thermal treatment. It appears that with thermal treatment, the $E_a$ is four times lower in the case of S removal with a value of 15 $kJ.mol^{-1}$. The decomposition of $MoS_2$ slabs requires lower activation energy than coke oxidation reaction ($E_a$= 60 $kJ.mol^{-1}$). The most important is the comparison with **NTP-R**, in which, there is a large drop in $E_a$ of C removal to 25 $kJ.mol^{-1}$ at only a $P_A$ of 2W, while it is not the case for S where $E_a$ at 2W is similar to thermal. As a function of $P_A$ of **NTP-R**, for both C and S, there is no significant difference as recognized in thermal, and $E_a$ exhibits a continuous decrease as a function of $P_A$ reaching values lower than

10 kJ.mol$^{-1}$ at higher $P_A$. It highlighted that the mechanism involved in C and S removals seems to be different between thermal treatment and **NTP-R**

The apparent activation energy for thermal regeneration is similar to that measured for the catalytic oxidation of light alkanes and aromatics (54-75 kJ.mol$^{-1}$) [31-34], and much lower than that of their pyrolysis, which occurs by C-C bond breaking ($E_a$ > 160 kJ mol$^{-1}$) [32]. Moreover, $E_a$ for NTP operating at moderate temperature is comparable to those measured for the attack of the oxygen radical on *n*-alkanes [34]:

$$n - C_xH_{2x+2} + O^{\circ} \longrightarrow n - C_xH_{2x+1}{}^{\circ} + HO^{\circ}, \qquad E_a = 7 - 16\ kJ.mol^{-1}.$$

These values suggest that the NTP oxidation mechanism follows a radical mechanism and initiates by breaking the C-H bond. The oxidation mechanism of thermal regeneration is different than the one occurring during NTP. **Figure 11a** supports this assumption, since it reports the product selectivity for both treatments by the plots of the yields into $CO_x$ as a function of the coke conversion. By extrapolating the beginnings of the plots, $CO_x$ seems to be the primary product in thermal treatment, while in **NTP-R** it is a secondary product. **Figure 11b** shows the molar ratio $CO_2$/CO versus the applied temperature at different PA. At low temperatures (<200 °C), the selectivity into $CO_2$ is much higher than CO, as indicated by the high ratio that reaches 25 mol/mol at 70 °C. While at high temperatures (> 200 °C), the molar ratio decreases, then becomes almost constant at 5 mol/mol regardless of the PA and equal to that of the thermal treatment.

XRD evidences $CoMoO_4$ formation even at 200°C under plasma discharge .

### 3.3. Comparison of the performances of the industrial (I-TR) and optimised thermal (O-TR) and to NTP regeneration (NTP-R) routes.

**Figure 12** compares the relative volumic activity (RVA) in toluene hydrogenation of regenerated catalyst by optimized thermal and NTP technologies; with the industrial regenerated catalyst activity being used as the reference (data supplied by IFPEN). Industrial, optimized thermal and non-thermal plasma regeneration are named **IT-R**, **OT-R**, and **NTP-R**, respectively. (**Table 1**) It is worth mentioning that results obtained on the NTP reactor (turn-off) and at the lab scale at IFPEN (OT-R) are similar (**Figure 3b**).

The Regeneration in an industrial unit eliminates coke but leads to undesirable $CoMoO_4$ species' formation due to hot spots. RVA increases in proportion to coke removal, suggesting that coke is rather located on the hydrogenating sites ($MoS_2$) than on the support ($Al_2O_3$). Yet, thermal regeneration, performed with different temperature plateaus, limits and even prevents at a lower temperature the formation of $CoMoO_4$.

This regeneration protocol improves the hydrogenation activity by 1.4 compared to the conventional industrial thermal regeneration. A substantial benefit (x 1.25) is obtained after **NTP-R** at 300 °C. Regardless of the applied power (3, 4, and 7 W) and the temperature used (200 and 300 °C), RVA after plasma regeneration at low temperature is also proportional to the coke elimination. The lower recovery efficiency of the hydrogenation activity by the **NTP-R** is not merely due to the presence of $CoMoO_4$. But probably to the modifications of the catalyst surface.

XPS characterizations were performed on the sulfide catalyst after toluene hydrogenation (**Figure 2**). **Table 1** compares the sulfidation rate and metal distribution with different coordination (Co Ox, S-Co, CoMoS) over catalysts regenerated using industrial and optimized thermal conditions and NTP at low temperatures. The NTP treatment leads to a slight increase in the molar ratios Mo/Al, suggesting a somewhat higher $MoS_2$ dispersion after non-thermal plasma regeneration than upon the optimized thermal treatment.

The advantage of NTP regeneration over thermal is the mitigation of oxide sintering. The ratios of (Co/Mo) sheets are similar on the catalysts after IT-R and **NTP-R**, but lower than after optimized thermal regeneration. The thermal regeneration optimization leads to better promotion of $MoS_2$ slabs by cobalt, consistent with a slightly higher % of CoMoS. The regeneration route has thus a real impact on the distribution of Co species after sulfiding treatment. The proportion of Co coordinated to a sulfur (Co-S) is significantly higher after **NTP-R** than after OT-R. Thus, cobalt no longer plays its role as a promoter, which harms the hydrogenation activity.

## Conclusion

The regeneration of the hydrodesulfurization catalyst is a challenge of great concern for oil refineries. The coke removal from an aged $CoMoP/Al_2O_3$ HDS industrial catalyst was studied using a non-thermal plasma reactor with coaxial geometry. NTP regeneration was carried out at a temperature ranging from 70 and 300 °C by applying power between 2 and 7W.

Complete removal of sulfur and coke is obtained under air from 400 °C but leads to the formation of undesirable species ($CoMoO_4$), which yields to an irreversible deactivation of the HDS catalyst. The apparent activation energies on coke and sulfur removal are 60 and 15 kJ. $mol^{-1}$, respectively.

At low temperature (< 150 °C and under non-thermal plasma (NTP) conditions), the oxidation efficiency of coke and sulfur is proportional to the power applied, but their removals remain partial. Complete regeneration of the catalyst requires the heating of the NTP reactor. Thus, the total elimination of sulfur and coke is obtained from 250 °C by applying only 3 W power. The apparent activation energy for coke removal is divided by more than three and becomes close to that encountered for the oxidation of hydrocarbon molecules by radical oxygen.

However, XRD evidences $CoMoO_4$ formation even at 200°C under plasma discharge. Catalytic performances and XPS characterization suggest that the modification of catalyst surface with the formation of new oxidic species other than $CoMoO_4$ is responsible for a lower quantity of CoMoS phase after plasma regeneration leading to the lower recovery efficiency of the NTP treated catalyst when compared to optimized isothermal oxidation (OT-R). Despite the presence of $CoMO_4$ and species of oxides preventing the cobalt from entirely playing its role as a promoter, the hydrogenation activity of regenerated HDS catalyst is higher than that obtained by conventional thermal regeneration in an industrial unit.

Non-thermal plasma regeneration is an alternative to the thermal route but still needs to be improved to avoid the formation of hot spots or maintain Co's promoter role. The oxidation of the catalyst surface must be controlled by adjusting the oxygen concentration in the feed gas, as in thermal regeneration optimization. Moreover, an optimization of the regeneration conditions (frequency variation, nature of the electrical signal, regeneration by sequences, etc.) should make it possible to achieve

the same performances as those obtained with optimized thermal regeneration. Moreover, the use of NTP for catalyst rejuvenation could also be considered.

**Acknowledgments:** The authors gratefully acknowledge IFPEN for the financial support. Hawraa Srour thanks the Lebanese University and IC2MP for the PhD grant. The authors acknowledge financial support from the European Union (ERDF) and "Région Nouvelle Aquitaine". The authors would be grateful to O. Delpoux and L. Lemaitre for the XPS analysis, S. Lopez for technical support in catalyst preparation and regeneration.

## References

[1] V. Rabarihoela-Rakotovao, F. Diehl, S. Brunet, Catal. Lett., 129 (2009) 50-60.

[2] J.A. Rob Van Veen, Catal. Today, 292 (2017) 2-25.

[3] C.H. Bartholomew, R.C. Reuel, Chem. Eng., 24 (1985) 56-61.

[4] J. H. Koh, J. J. Lee, H. Kim, A. Cho et S. H. Moon, Appl. Catal. B: Environ., 86 (2009) 176–181.

[5] B. Guichard, M. Roy-Auberger, C. Pichon, Appl. Catal. A, 367 (2009) 9-22.

[6] Y. Yoshimura, T. Sato, H. Shimada, N. Matsubayashi, Energy & Fuels, 8 (1994) 435-445.

[7] N.-Q. Bui, C. Geantet, G. Berhault, J. Catal., 330 (2015) 374-386.

[8] A. Pimerzin, A. Roganov, A. Mozhaev, K. Maslakov, P. Nikulshin, A. Pimerzin Fuel Processing Technology 173 (2018) 56–65.

[9] N.-Q. Bui, C. Geantet, G. Berhault, Applied Catalysis A, General 572 (2019) 185–19.

[10] Y. Liu, S. Lu, X. Yan, S. Gao, X. Cui, Z. Cui, Journal of Cleaner Production 256 (2020) 120422

[11] A. Pathak, M. Vinoba, R. Kothari, Richa, Crit. Rev. Env. Sc. Tech. 51 (2021) : 1-43.

[12] A. Bogaerts, X. Tu, C. Xhiteheas, G. Centi, L. Lefferts, O. Guaitella, F. Assolina-Jury, H.-H. Kim, A. B. Murphy, W. F. Schneider, T. Nozaki, J. C. Hicks, A. Rousseau, F. Thevenet, A. Khacef, M. Carreon, J. Phys. D: Appl. Phys. (2020) **53** 443001

[13] D.H. Lee, Y.H. Song, K.T. Kim, S.Jo, H. Kang, Catal. Today, 337 (2019) 15-27.

[14] B. Eliasson, M. Hirth, U. Kogleschatz, J. Phys. D. Appl. Phys., 20 (1987) 1421-1437.

[15] Y. Fan, Y. Cai, X. Li, H. Yin, L. Chen, S. Liu, J. Anal. Appl. Pyro, 111 (2015) 209-215.

[16] N. Hafez Khiabani, S. Fathi, B. Shokri, S. I. Hosseini, Appl. Catal. A : Gen, 493 (2015) 8-16.

[17] L. Jia, Al Farouha, L. Pinard, S. Hedan, J. -D Comparot, A. Dufour, K. Ben Tayeb, H. Vezin, C. Batiot-Dupeyrat, Appl. Catal. B: Env, 219 (2017) 82-91.

[18] L. Pinard, N. Ayoub et C. Batiot-Dupeyrat, Plasma Chem. and Plasma Process., 239-4 (2019) 929-936.

[19] H. Srour, A. Alnaboulsi, A. Astafan, E. Devers, J. Toufaily, T. Hamieh, L. Pinard, C. Batiot-Dupeyrat, Catalysts, 9 (2019) 783-800.

[20] A. Astafan, C. Batiot-Dupeyrat, L. Pinard, J. Phys. Chem. C, 123 (14) (2019) 9168-9175.

[21] A. H. Khoja, M. Tahir et N. A. S. Amin, Energy Conv. and Manag., 144 (2017) 262–274.

[22] M. S. Gandhi , Y. S. Mok, J. Env. Sci.., 24(7) (2012) 1234–1239.

[23] S. K. Kundu, E. M. Kennedy, V. V. Gaikwad, T. S. Molloy, Bogdan Z. Dlugogorski, Chem. Eng. J., 180 (2012) 178–189.

[24] M. Hołub, Int. J. of Appl. Electromagnetics and Mechanics, 39 (2012) 81–87.

[25] A. D. Gandubert, C. Legens, D. Guillaume, S. Rebours, E. Payen, Oil Gas Sci.Technol. 62 (2007) 79- 83.

[26] A. D. Gandubert, C. Legens, D. Guillaume, E. Payen, Surf. Inter. Anal. 38 (2006) 206-209

[27] G. Perot, Catal. Today 86 (2003) 111-128.

28] M. Marafi, A. Stanislaus , Appl.Catal. A: Gen., 159 (1997) 259-267.

[29] P.D. Hopkins et B.L. Meyers, Ind. Eng. Chem., Prod. Res. Dev., 3 (1983) 421-426.

[30] B. Pietruska, M. Heintze, Catal. Today, 90 (2004) 151-158.

[31] M. Aryada , F. Zaera, Catal. Lett., 48 (1997) 173-183.

[32] T. F. Garetto, C. R. Aspeteguia,. Appl Catal. B: Env.l, 32 (2001) 83-94.

[33] A; Ristori, P. Dagaut, M. Cathonnet, Combust Flame, 125 (2001) 1128-1137.

[34] W. Mayer, L. Schieler, J. Phys Chem, 73 (1968) 2628-2631.

**Figure and table captions**

Table 1: Operating conditions of industrial and optimised thermal regeneration processes and non-thermal plasma at low temperature. Sulfidation rate and metals repartition by XPS over catalyst after toluene hydrogenation

Figure 1: Dielectric barrier discharge plasma reactor.

Figure 2: Deconvolution XPS spectra of MO (a), Co (b) and S (c) elements.

Figure 3: (a) Cumulative yield into $CO_x$ as a function of time at different regeneration temperatures: 320, 350, 380, and 450 °C, and (b) the relative C and S removals after 64 minutes.

Figure 4**:** XRD patterns of spent catalyst before (a) and after thermal regeneration at 200 (b), 300 (c) and 500°C (d), in blue after plasma treatment at 200°C with 7W.

Figure 5: TEM images of spent catalyst before after thermal regeneration during 30minutes at 500 °C

Figure 6: Impact of temperature on deposited power (P):

**(a)** P at different temperatures: 70, 150, 200 and 300°C as a function of the applied voltage;

**(b)** Applied voltage (U) required to obtain a deposited power of 3, 4, 5, 6 and 7W as a function of the temperature.

Figure 7: Impact of temperature on the efficiency of non-thermal plasma on: (**a,b**) carbon and sulfur removal, **(c)** cumulated conversion to COx ($CO_2$+CO), (**d)** carbon balance and comparison with thermal regeneration (Full symbol). Results obtained after 1h regeneration at different applied powers (2, 3, 4, 5, 6 and 7W).

Figure 8: Impact of applied power (P) on the efficiency of non-thermal plasma on (**a,b**) carbon and sulfur removal, **(c)** cumulated conversion to COx ($CO_2$+CO), (**d)** carbon balance. Results obtained after 1h regeneration at different temperatures: 70, 150, 200 and 300 °C.

Figure 9: Temperature dependency of removal of carbon **(a)** and sulfur **(b)** and apparent activation energy ($E_a$) as a function of the applied power; Results obtained after 1h regeneration.

Figure 9: Temperature dependency of removal of carbon **(a)** and sulfur **(b)** as a function of the applied power; Results obtained after 1h regeneration.

Figure 10: apparent activation energy ($E_a$) as a function of the applied power; Results obtained after 1h regeneration.

Figure 11: Selectivity of NTP process:

**(a)** Cumulated yield into $CO_x$ as a function of coke conversion drawn from elementary analysis,

**(b**) Molar ratio of $CO_2$/CO at different applied power as a function of temperature.

Figure 12: Relative Volumic Activity of toluene hydrogenation (the industrial regenerated catalyst activity being the reference) of spent catalyst (●) and regenerated catalysts by IT-R (◆), O-TR ( □) and NTP-R (△) processes.

**Supporting Information**

Fig. SI. 1 Lissajous figure for P=5W at 70, 150, 200 and 300°C during plasma treatment

**Table 1:** Operating conditions of industrial and optimised thermal regeneration processes and non-thermal plasma at low temperature. Sulfidation rate and metals repartition by XPS over catalyst after toluene hydrogenation.

| Regeneration Mode | T (°C) | P (W) | Removal of (%) | | Presence of $CoMO_4$[a] | Mo/Al | Co/Al | $(Co/Mo)_{sheet}$[b] | SR[c] (%) | Co repartition (rel.%) | | |
|---|---|---|---|---|---|---|---|---|---|---|---|---|
| | | | C | S | | Mol/Mol | | | | $Co^{2+}$ | Co-S | CoMoS |
| I-TR | 450 | | 100 | 94.8 | +++ | 0.31 | 0.08 | 0.25 | 73.3 | 36.2 | 21 | 43 |
| O-TR | 300 | | 7.4 | 87.8 | | 0.28 | 0.08 | 0.31 | 78.4 | 32.6 | 18 | 50 |
| | 320 | | 56.0 | 94.6 | Traces | 0.33 | 0.10 | 0.31 | 76.6 | 34.4 | 16 | 50 |
| | 350 | | 81.6 | 99.0 | + | 0.30 | 0.08 | 0.30 | 76.7 | 34.9 | 14 | 51 |
| | 450 | | 99.6 | 100 | + | 0.37 | 0.08 | 0.29 | 75.5 | 40.6 | 12 | 48 |
| NTP-R | 200 | 4 | 54.2 | 66.2 | Traces | 0.37 | 0.11 | 0.31 | 77.8 | 28.0 | 24 | 48 |
| | 200 | 7 | 99.9 | 99.9 | + | 0.34 | 0.09 | 0.26 | 79.4 | 29.9 | 23 | 47 |
| | 300 | 3 | 98.8. | 97.9. | + | 0.34 | 0.09 | 0.24 | 78.1 | 32.6 | 25 | 43 |

[a] detected by XRD, [b] Co/Mo in the sheets calculated according to Eq. 3,, [c]Sulfitation rate calculated according to Eq. 2

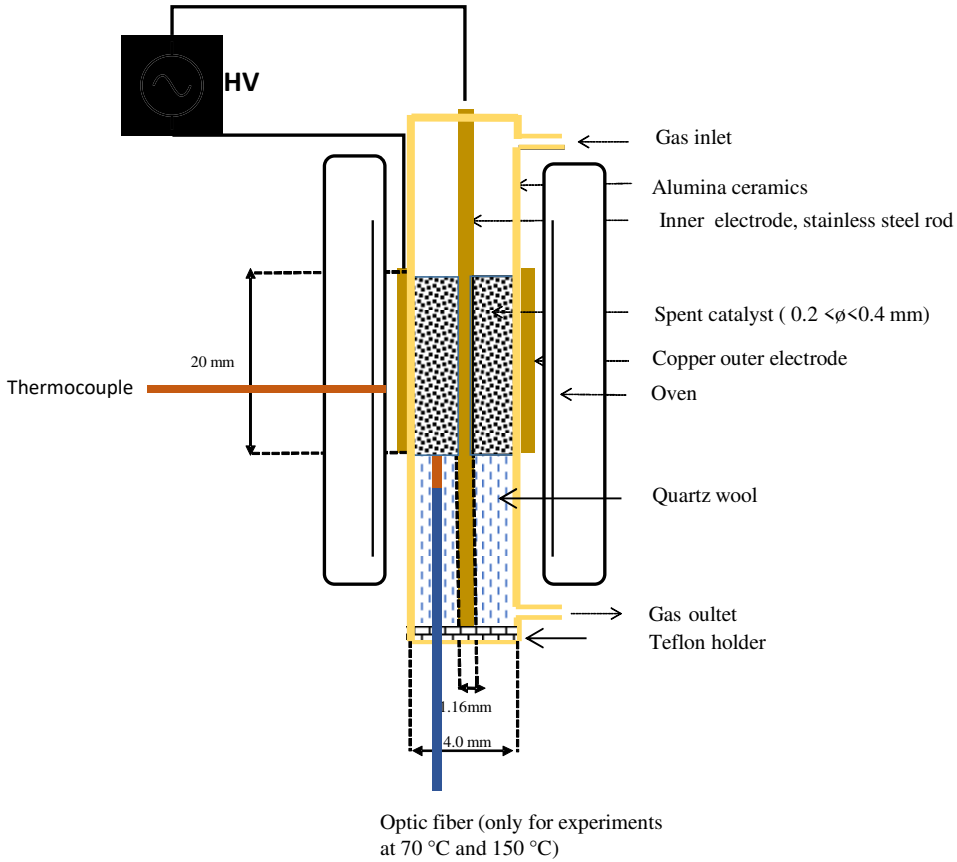


**Figure 1**: Dielectric barrier discharge plasma reactor

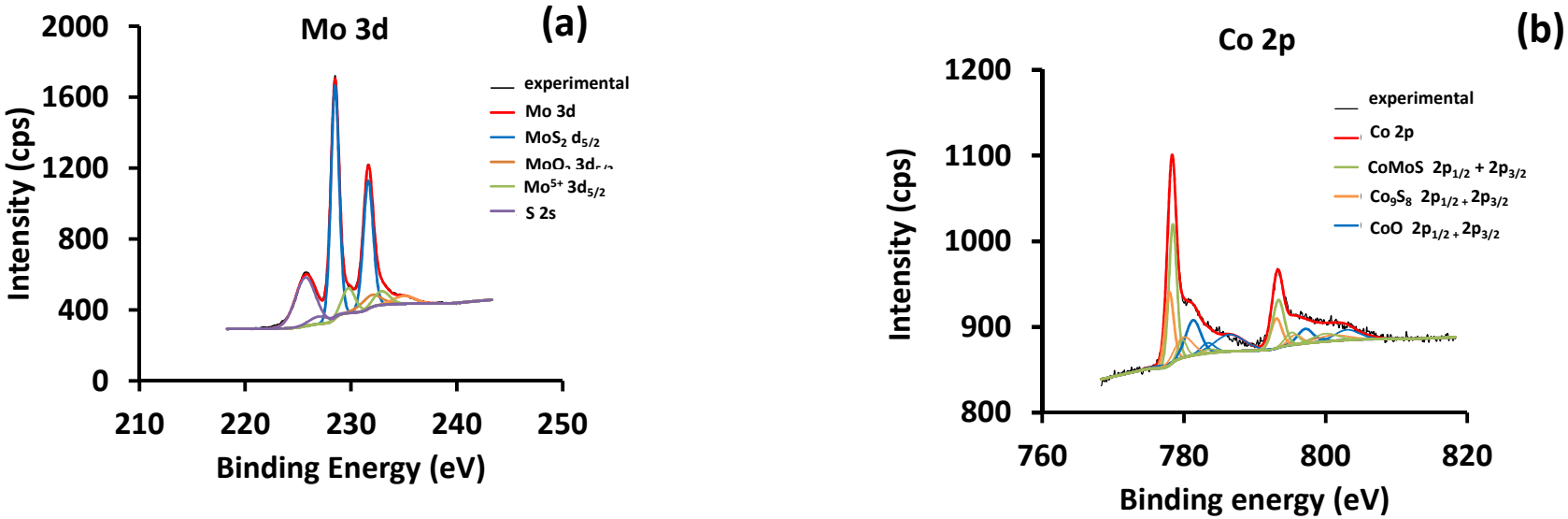


**Figure 2:** XPS spectra of after toluene hydrogenation: cobalt and molybdenum elements.

(a)

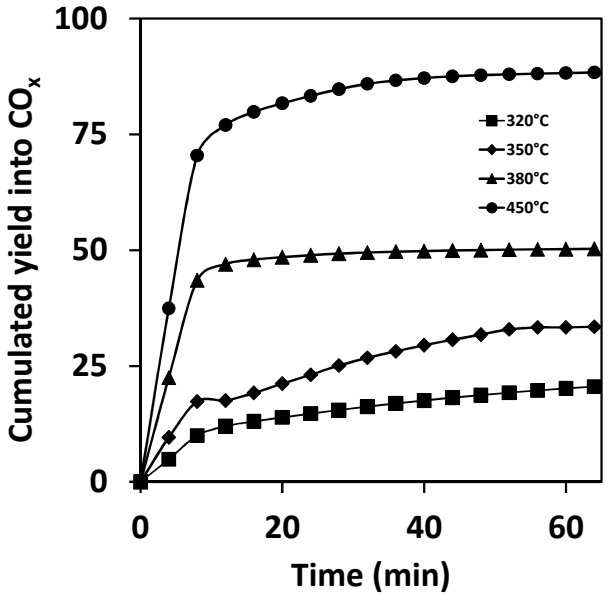
100
75
50
25
0
0
20
40
60
Time (min)
Cumulated yield into $CO_x$
320°C
350°C
380°C
450°C

(b)

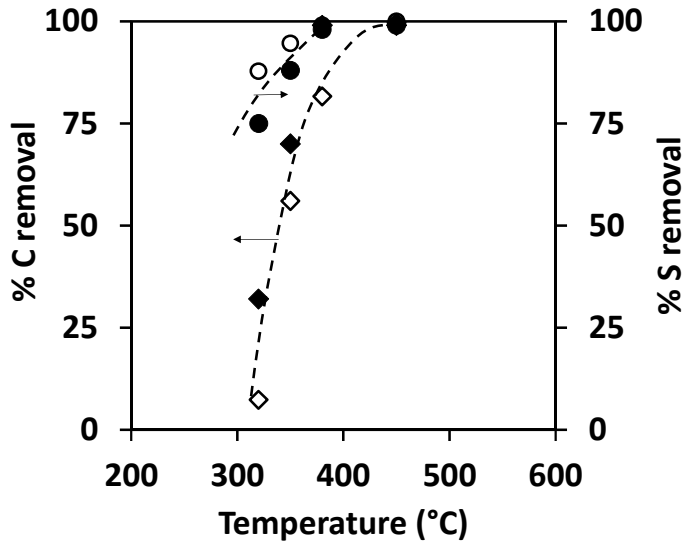
100
75
50
25
0
200
300
400
500
600
Temperature (°C)
% C removal
% S removal

**Figure 3:** (a) Cumulative yield into $CO_x$ as a function of time at different regeneration temperatures: 320, 350, 380, and 450°C, and (b) the relative C and S removals after 64 minutes. Full symbol regeneration carried out in the NTP reactor (turn-off) (**$TR_{DBD\ reactor}$**) , open symbol: regeneration at the lab scale (**O-TR**),

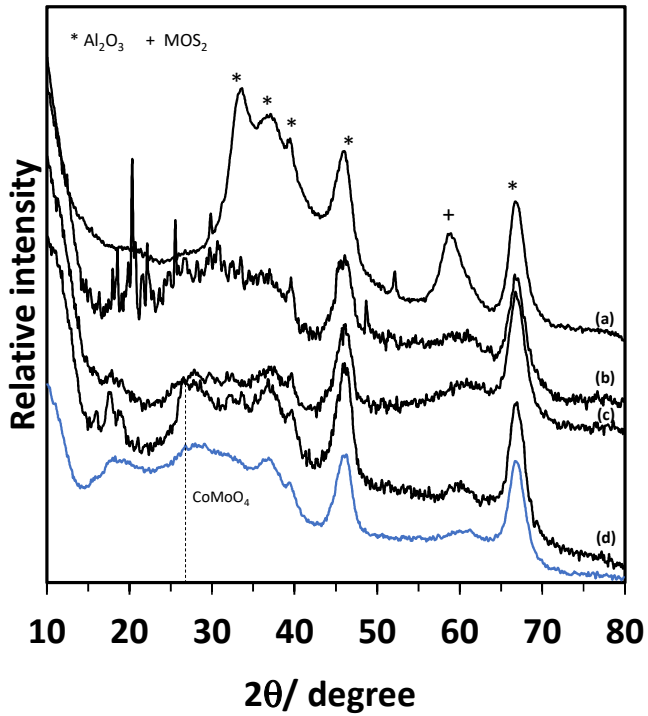


**Figure 4:** XRD patterns of spent catalyst before (a) and after thermal regeneration during 30 min at 200 (b), 300 (c) and 500°C (d). in blue after plasma treatment at 200°C with 7W

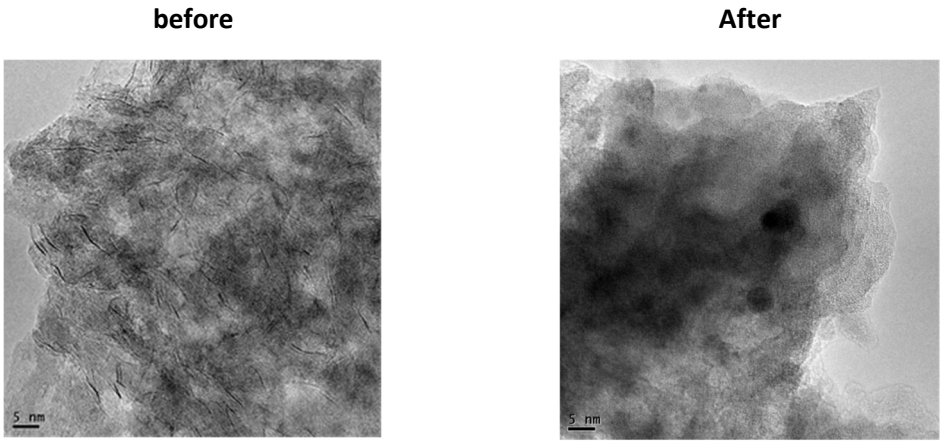


**Figure 5:** TEM images of spent catalyst before after thermal regeneration during 30mins at 500 °C

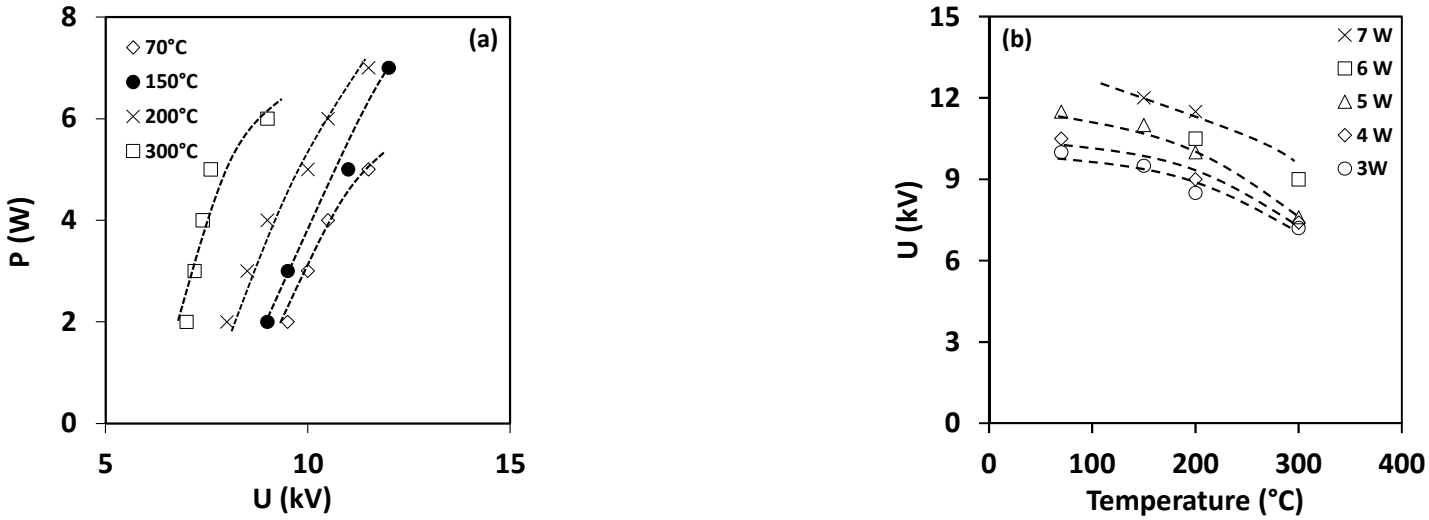


**Figure 6:** Impact of temperature on deposited power (P): **(a)** P at different temperatures: 70, 150, 200 and 300°C as a function of the applied voltage; **(b)** Applied voltage (U) required to obtain a deposited power of 3, 4, 5, 6 and 7W as a function of the temperature

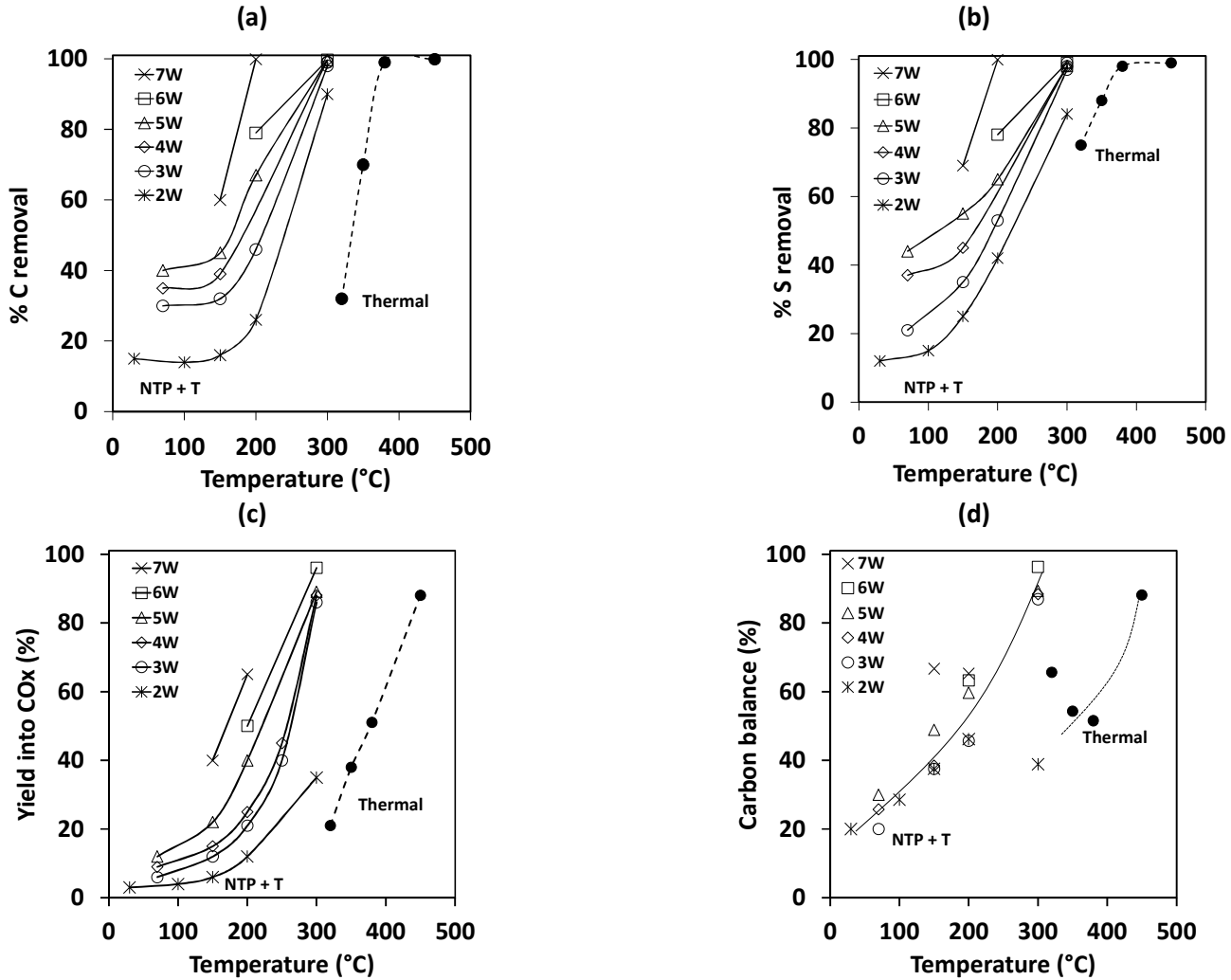


**Figure 7**: Impact of temperature on the efficiency of non-thermal plasma on: (**a,b**) carbon and sulfur removal, **(c)** cumulated conversion to COx ($CO_2$+CO), (**d)** carbon balance and comparison with thermal regeneration (Full symbol). Results obtained after 1h regeneration at different applied powers (2, 3, 4, 5, 6 and 7W);

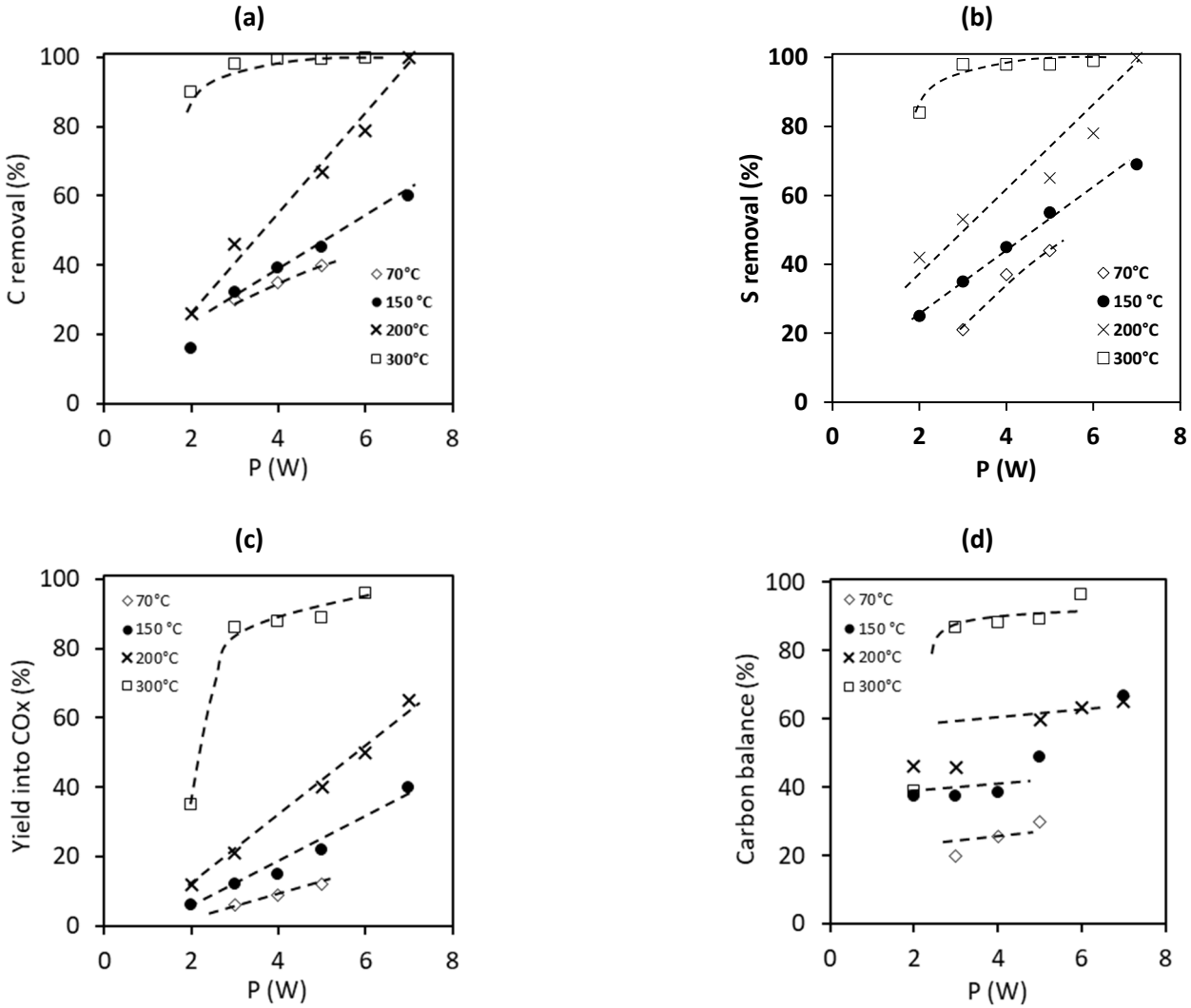
(a)
C removal (%)
P (W)
70°C
150 °C
200°C
300°C
(b)
S removal (%)
P (W)
70°C
150 °C
200°C
300°C
(c)
Yield into COx (%)
P (W)
70°C
150 °C
200°C
300°C
(d)
Carbon balance (%)
P (W)
70°C
150 °C
200°C
300°C

**Figure 8:** Impact of applied power (P) on the efficiency of NTP on (**a,b**) carbon and sulfur removal, **(c)** cumulated conversion to COx ($CO_2$+CO), (**d)** carbon balance. Results obtained after 1h regeneration at different temperatures: 70, 150, 200 and 300°C.

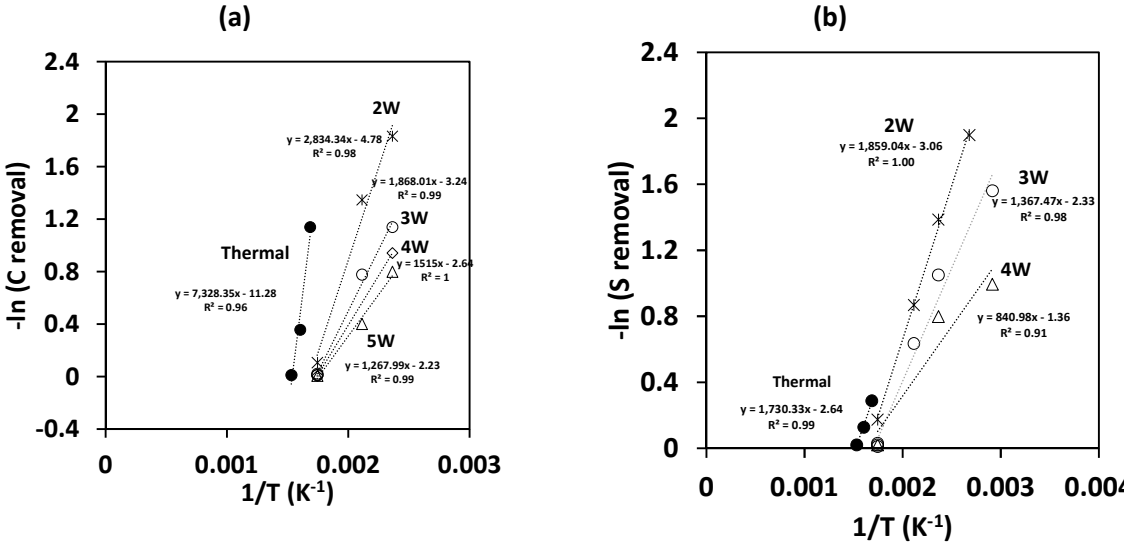


**Figure 9:** Temperature dependency of removal of carbon (a) and sulfur (b) as a function of the applied power. Results obtained after 1h regeneration

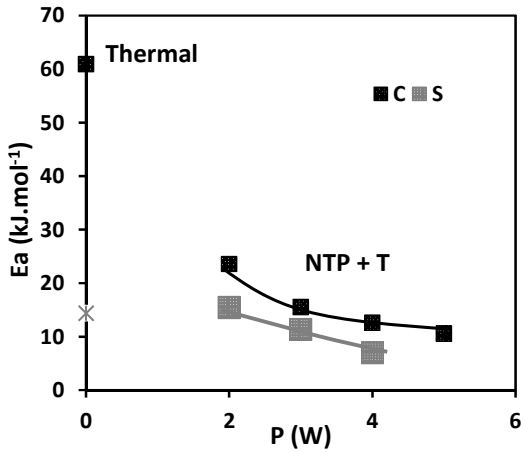


**Figure 10:** Aapparent activation energy (Ea) as a function of the applied power. Results obtained after 1h regeneration

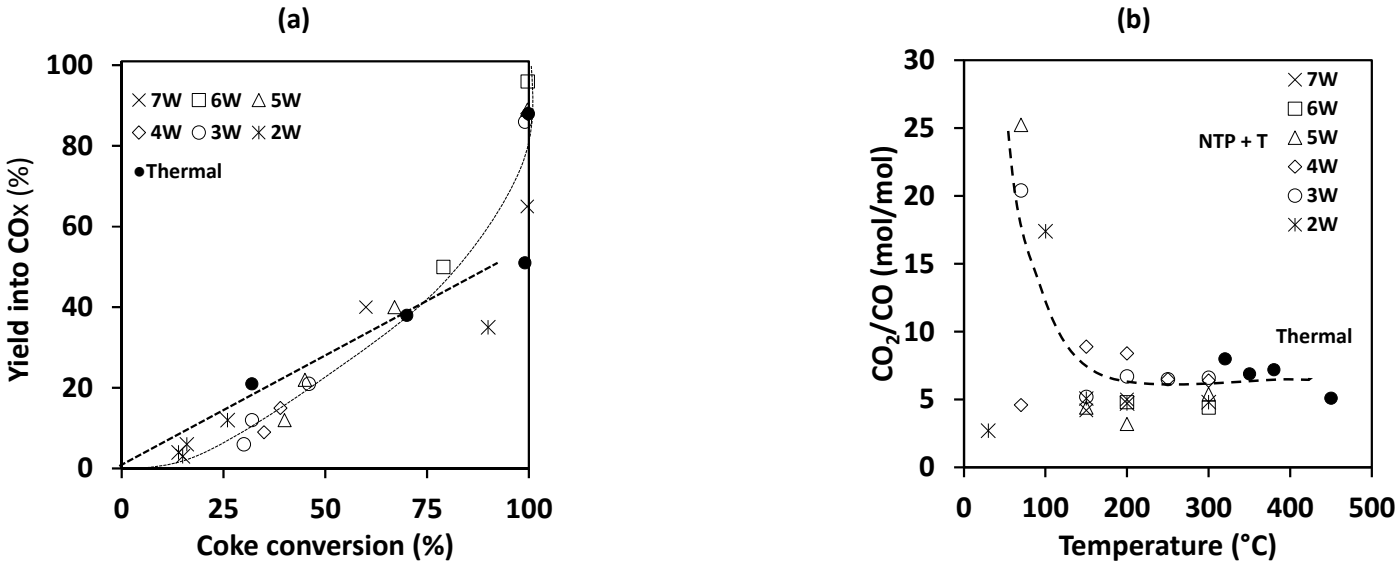


**Figure 11**: Selectivity of NTP process:

**(a)** Cumulated yield into Cox after 1h as a function of coke conversion drawn from elementary analysis,

**(b**) Molar ratio of $CO_2$/CO at different applied power as a function of temperature

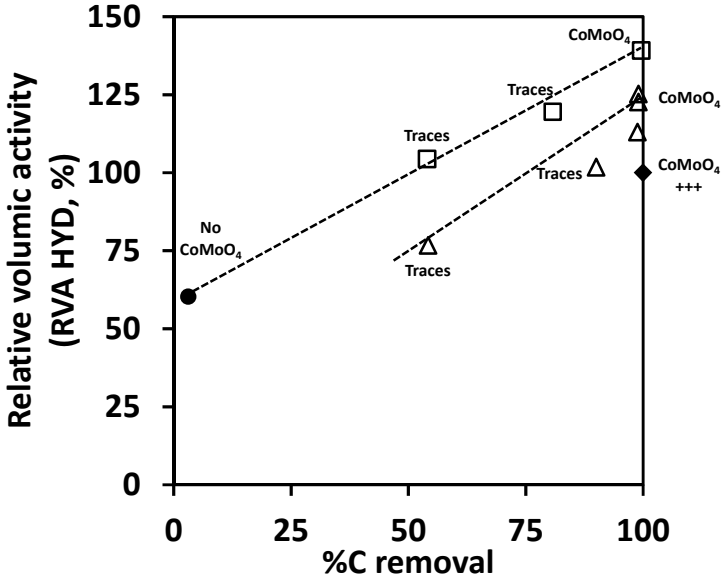


**Figure 12**: Relative Volumic Activity of toluene hydrogenation (the industrial regenerated catalyst activity being the reference) of spent catalyst (●) and regenerated catalysts by IT-R (◆), OTR ( □) and NTP-R (△) processes.

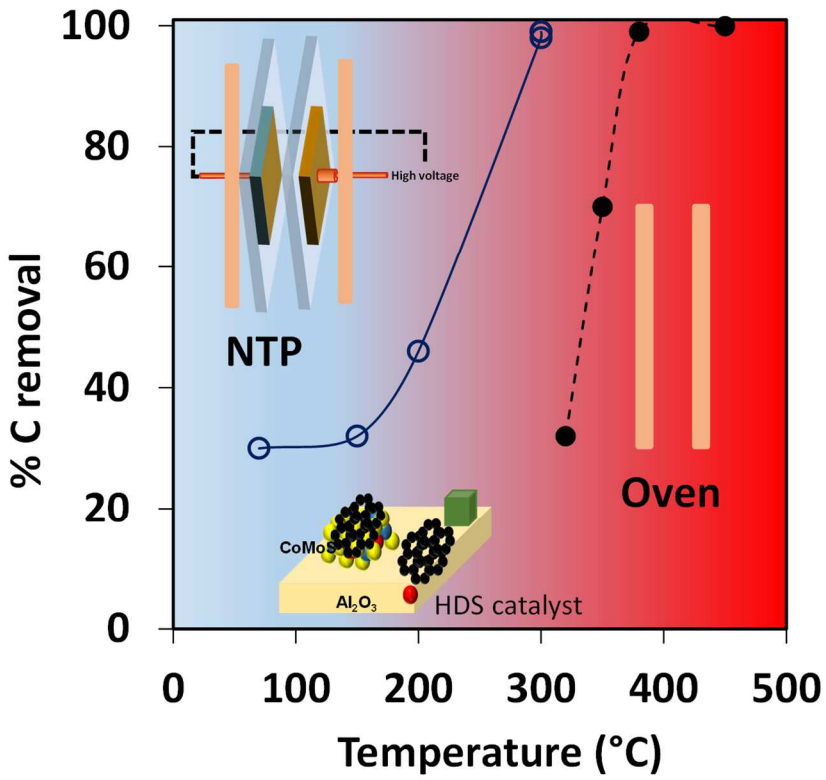
100
80
60
40
20
0
% C removal
0
100
200
300
400
500
Temperature (°C)
High voltage
NTP
Oven
CoMoS
$Al_2O_3$
HDS catalyst